Cancer Research

Requirement of the NF-κB Subunit p65/RelA for K-Ras–Induced Lung Tumorigenesis

Daniela S. Bassères[1], Aaron Ebbs[1], Elena Levantini[3], and Albert S. Baldwin[1,2]

Abstract

K-Ras–induced lung cancer is a very common disease, for which there are currently no effective therapies. Because therapy directly targeting the activity of oncogenic Ras has been unsuccessful, a different approach for novel therapy design is to identify critical Ras downstream oncogenic targets. Given that oncogenic Ras proteins activate the transcription factor NF-κB, and the importance of NF-κB in oncogenesis, we hypothesized that NF-κB would be an important K-Ras target in lung cancer. To address this hypothesis, we generated a NF-κB-EGFP reporter mouse model of K-Ras–induced lung cancer and determined that K-Ras activates NF-κB in lung tumors *in situ*. Furthermore, a mouse model was generated where activation of oncogenic K-Ras in lung cells was coupled with inactivation of the NF-κB subunit p65/RelA. In this model, deletion of p65/RelA reduces the number of K-Ras–induced lung tumors both in the presence and in the absence of the tumor suppressor p53. Lung tumors with loss of p65/RelA have higher numbers of apoptotic cells, reduced spread, and lower grade. Using lung cell lines expressing oncogenic K-Ras, we show that NF-κB is activated in these cells in a K-Ras–dependent manner and that NF-κB activation by K-Ras requires inhibitor of κB kinase β (IKKβ) kinase activity. Taken together, these results show the importance of the NF-κB subunit p65/RelA in K-Ras–induced lung transformation and identify IKKβ as a potential therapeutic target for K-Ras–induced lung cancer. *Cancer Res; 70(9); 3537–46. ©2010 AACR.*

Introduction

Lung cancer is the second most common type of cancer in the United States, yet it is the leading cause of cancer deaths (1). Importantly, activating point mutations in the K-Ras GTPase gene occur in a large number of lung cancer patients (2–4). These mutations not only are associated with poor prognosis and therapy resistance (5, 6) but also have been causally linked to the oncogenic process. In this regard, expression of mutant K-Ras in mice is sufficient to cause transformation and tumor formation (7, 8). Effective abrogation of K-Ras activity reverts malignant cells to a nonmalignant phenotype (9–12). Therefore, cancer therapy targeting K-Ras would be expected to produce a clinical benefit. Unfortunately, therapies aimed at inhibiting the biological activity of K-Ras have thus far been unsuccessful (13). In order for more effective therapies for K-Ras–induced lung cancer to be generated, the critical K-Ras effectors involved in oncogenesis need to be identified.

The transcription factor NF-κB is a dimeric complex formed by members of a conserved family of proteins that share a motif, designated as the Rel homology domain. NF-κB is expressed ubiquitously, and the primary NF-κB member responsible for transcriptional activation of target genes is the subunit p65/RelA (14, 15). In unstimulated nontransformed cells, most NF-κB complexes are held in an inactive cytoplasmic form through interactions with the inhibitor of κB (IκB) proteins. Upon stimulation with cytokines or other relevant molecules, IκB is phosphorylated by the IκB kinase (IKK) complex and undergoes rapid ubiquitination and proteasome-mediated degradation. The NF-κB subunits are then released and accumulate in the nucleus to regulate target gene transcription (14, 15).

Although NF-κB has been reported to have a tumor-suppressive role in certain specific settings (16), the majority of studies show that, when activated, NF-κB can contribute to oncogenic transformation (17). Indeed, NF-κB is important for cellular transformation induced by oncoproteins (18, 19). Not surprisingly, constitutive NF-κB activation has been detected in a variety of human malignancies (17), including lung cancer (20).

Importantly, NF-κB is activated by oncogenic Ras. Studies from our group revealed that oncogenic H-Ras induces cellular transformation in fibroblasts by activating NF-κB (18), and NF-κB activation is required to suppress oncogenic H-Ras–induced apoptosis (21). Other studies have shown a correlation between increased NF-κB activity and expression

Authors' Affiliations: [1]Lineberger Comprehensive Cancer Center and [2]Department of Biology, University of North Carolina, Chapel Hill, North Carolina and [3]Beth Israel Deaconess Medical Center, Harvard Medical School, Boston, Massachusetts

Note: Supplementary data for this article are available at Cancer Research Online (http://cancerres.aacrjournals.org/).

Corresponding Author: Albert S. Baldwin, Lineberger Comprehensive Cancer Center, University of North Carolina, 450 West Drive, CB#7295, Chapel Hill, NC 27599-7295. Phone: 919-966-3652; Fax: 919-966-8212; E-mail: albert_baldwin@med.unc.edu.

doi: 10.1158/0008-5472.CAN-09-4290

©2010 American Association for Cancer Research.

Downloaded from http://aacrjournals.org/cancerres/article-pdf/70/9/3537/2653977/3537.pdf by guest on 29 April 2025

of oncogenic K-Ras (20, 22). Duran and colleagues (23) showed a mechanistic link between K-Ras, IKK, and NF-κB through the signaling adaptor p62. Based on these cell-based studies, it is important to determine if NF-κB is required for development of K-Ras–induced tumors *in situ*.

Here, we show that oncogenic K-Ras activates NF-κB in lung epithelial cells *in situ*. In addition, genetic deletion of the NF-κB subunit p65/RelA in a K-Ras–induced lung cancer mouse model reduces lung tumorigenesis both in the presence and in the absence of the tumor suppressor p53. K-Ras–dependent NF-κB activity was observed in transformed human lung epithelial cells. Interestingly, NF-κB activity in both murine and human K-Ras–transformed cells requires IKKβ kinase activity. These results show NF-κB (p65/RelA) as an important K-Ras oncogenic effector in lung cancer and suggest pharmacologic inhibition of IKKβ activity as a therapeutic approach for K-Ras–related malignancies.

Materials and Methods

Animal husbandry and Cre-expressing adenovirus administration. Lox-stop-lox (LSL) K-Ras^{G12D} mice (24), *cis*-κB-EGFP mice (25), p65/RelA conditional mice (26), p53 conditional mice (27), and mice generated by interstrain crossings were housed in pathogen-free conditions according to the protocols approved by the University of North Carolina Institutional Animal Care and Use Committee. Lung tumor induction was performed by intranasal administration of 1×10^7 plaque-forming units of Cre-expressing adenovirus (adenocre; Gene Transfer Vector Core, University of Iowa, Iowa City, IA) in selected animals at 8 weeks of age, as described (24).

Histopathologic analysis. Mice were euthanized by i.p. administration of 250 mg/kg Avertin followed by surgical resection of the portal vein. Lungs were perfused with saline and inflation fixed overnight with 10% formalin. Fixed tissues were embedded in paraffin, sectioned at 5-μm thickness, and stained with H&E.

Live imaging and laser scanning microscopy. The whole-body small-animal fluorescence imaging system (Xenogen IVIS 100 system, Caliper Life Sciences) equipped with a charge-coupled device (CCD) camera was used to visualize green fluorescent protein (GFP) fluorescence emission using GFP filter for excitation (445–490 nm) and emission (515–575 nm). Analysis of the images was performed using Living Image software (Caliper Life Sciences). Laser scanning microscopy was performed using a Nipkow-type spinning disk confocal scan head (CSU-10, Yokogawa Corp.) with a 10× objective, attached to an inverted microscope (model IX-81, Olympus). Images were acquired using a CCD camera (model C4742-80-12AG, Hamamatsu).

Western blotting and immunohistochemistry. Western blotting and immunohistochemistry were performed as described (26, 28). The antibodies used were as follows: anti–phospho-IκBα-Ser$^{32/36}$, anti-IκBα, anti–phospho-AKT-Ser^{473}, anti–phospho-p44/42-mitogen-activated protein kinase (MAPK)-Thr^{202}/Tyr^{204}, anti–p44/42-MAPK, anti–phospho-IKKα/β-Ser$^{176/180}$, and anti-p65/RelA antibodies (Cell Signaling); anti–pan-Ras^{12D} and anti–c-K-Ras (Calbiochem); anti-GFP (Clontech); anti–β-tubulin (Santa Cruz Biotechnology); and anti-IKKβ (Chemicon).

Detection of Cre-mediated recombination. Cre-mediated recombination of the p65 conditional allele was detected by PCR amplification with primers flanking the deleted site (sequences available on request). Amplification of the wild-type (WT) allele results in a 3.9-kb product, and amplification of the deleted allele results in a 1.3-kb product. Amplification was performed by denaturation at 95°C for 1 minute, followed by 35 cycles of amplification at 98°C for 10 seconds, 52°C for 30 seconds, and 72°C for 90 seconds, with a final extension step of 10 minutes at 72°C.

Terminal deoxynucleotidyl transferase–mediated dUTP nick end labeling assay. Tissue sections were deparaffinized, rehydrated, and stained according to the ApopTag Plus *In Situ* Apoptosis Detection kit (Millipore) instructions.

Tumor number and grade analysis. Tumor slides from each lung lobe (same orientation and level section used for each lobe) were scored for number, spread, and grade blindly. For analysis of tumor spread, tumors were divided into either bronchial lesions or alveolar lesions according to the following criteria. Bronchial lesions were either tumor masses completely contained within the bronchial compartment or lesions where the spread into the alveolar compartment was smaller than the bronchial component. Alveolar lesions were either lesions restricted to the alveolar compartment (excluding adenomatous alveolar hyperplasia) or lesions where the alveolar spread was larger than the bronchial component (including solid tumors). For analysis of tumor grade, each tumor was given a score of 1 to 5 based on previously described criteria (29).

Generation of KE67 cell line. Lung tumors from K-Ras/NF-κB mice were dissected under aseptic conditions and cut into small pieces (~2 mm in diameter). Each piece was placed in a 100-mm cell culture dish with 2 mL of 0.25% trypsin-EDTA (Invitrogen) and minced with a sterile razor blade. After trypsinization, 8 mL of complete medium were added to the dish and cells were transferred to 15-mL conical tubes. Untrypsinized tumor chunks and tissue debris were allowed to sediment for 10 minutes. Both the supernatant and sedimented fractions were collected and plated separately in 100-mm dishes. Cells were then kept on culture and passed when confluency was reached. To inhibit fibroblast growth, the culture medium was supplemented with Mouse FibrOut 9 (Chi Scientific) for a week.

Cell culture. Cell passages were kept to a minimum, and no cells were passaged continuously for >6 months. Low-passage SALEB and SAKRAS cells were obtained from Dr. Scott Randell and cultured in serum-free bronchial epithelium growth medium (Clonetics-Lonza). These cells were originally selected in medium containing a triple antibiotic cocktail and subsequently characterized by real-time PCR for expression of the genes used for immortalization and transformation (30). Short tandem repeat DNA profile authenticated NCI-H358 cells were obtained from the American Type Culture Collection and maintained in RPMI 1640 (Invitrogen) supplemented with 10% fetal bovine serum

Downloaded from http://aacrjournals.org/cancerres/article-pdf/70/9/3537/2653977/3537.pdf by guest on 29 April 2025

(FBS; Sigma-Aldrich). KE67 cells were generated in the laboratory (as described above), and their origin was authenticated both by PCR of the excised K-Ras allele and by expression of enhanced GFP (EGFP) from the reporter allele. They were maintained in DMEM (Invitrogen) supplemented with 10% FBS and 0.5 mmol/L 2-mercaptoethanol (both from Sigma-Aldrich).

Electrophoretic mobility shift assay. Cells were either transfected or treated with appropriate reagents, nuclear extracts were prepared, and electrophoretic mobility shift assay (EMSA) was performed as previously described (28) using ^{32}P-labeled oligonucleotide probes corresponding to a NF-κB site within the MHC class I promoter region.

RNA isolation and real-time PCR analysis. Total RNA was prepared using Trizol reagent (Invitrogen) following the manufacturer's protocol, and real-time PCR analysis was performed as previously described (28) in an ABI 7000 Sequence Detection System using Taqman Gene Expression Assay primer-probe sets (all from Applied Biosystems) for *interleukin-8* (*IL-8*; Hs99999034_m1), *Bcl-XL* (Hs00236329_m1), and *matrix metalloproteinase-9* (*MMP-9*; Hs00234579_m1). Relative quantitation was determined by the $\Delta\Delta C_t$ method using Gusb (Hs99999908_m1) as the endogenous control.

Transfections and reporter assays. Small interfering RNA (siRNA) transfections were performed as previously described (28) with 100 nmol/L of either a nontargeting siRNA control or siRNA smart pools targeting IKKβ or K-Ras (Dharmacon). Reporter assays were performed as described (28). For genetic studies, cells were cotransfected with 100 ng of either empty pcDNA3 vector (Invitrogen) for control or a pcDNA3 vector encoding the kinase mutant form of IKKβ (IKKβ-KM). For pharmacologic studies, cells were treated as indicated (see figure legends). Relative light units were measured on an LMax Microplate Luminometer (Molecular Devices).

Flow cytometry. KE67 cells (2×10^5) plated in six-well plates were treated with either 0.1% DMSO or 5 μmol/L IKKβ inhibitor CmpdA (31) for 16 hours. Cells were then scraped in PBS supplemented with 2% FBS and subsequently analyzed for GFP expression on a Beckman-Coulter Cyan ADP cytometer (Dako). Results were analyzed with FlowJo software (Tree Star).

Statistics. All values are presented either as mean ± SD or as representative images of at least three independent experiments. In the case of animal studies, five mice of each different genotype were analyzed. All comparisons were made using the unpaired Student's *t* test for samples with unequal variance. Differences were considered statistically significant at $P \leq 0.05$ (indicated by asterisks).

Results

Generation of a NF-κB reporter mouse model of K-Ras–induced lung cancer. To determine if NF-κB activity is induced in mouse lung tumors triggered by activation of oncogenic K-Ras, a NF-κB reporter mouse model of K-Ras–induced lung cancer was developed. To generate this model, we used oncogenic K-Ras–inducible LSL K-Ras^{G12D} mice (24), where expression of oncogenic K-Ras^{G12D} is triggered by Cre recombinase-mediated removal of the LSL element. The LSL K-Ras^{G12D} mice were then bred to *cis*-NF-κB-EGFP knock-in mice, which express EGFP under the control of NF-κB *cis* elements (25). Mice positive for the conditional K-Ras allele and the NF-κB–responsive EGFP reporter allele (referred to as K-Ras^{G12D}/NF-κB mice) were infected by intranasal administration of adenocre to activate oncogenic K-Ras^{G12D} specifically in lung epithelial cells and induce lung tumor formation.

NF-κB is activated in mouse K-Ras–induced lung cancers. NF-κB activity in K-Ras^{G12D}/NF-κB mice was evaluated by measuring the levels of EGFP expression in the lungs of tumor-bearing animals. First, noninvasive live fluorescence imaging was used to measure EGFP expression at 19 weeks postinfection when lung adenocarcinomas can be detected (24). As can be seen in Fig. 1A, K-Ras^{G12D}/NF-κB mice have higher EGFP fluorescence emission levels in the chest area than K-Ras^{WT}/NF-κB mice (mice positive for the NF-κB–responsive EGFP reporter allele but lacking the conditional K-Ras allele). Next, EGFP expression was measured directly in dissected lungs by laser scanning fluorescence microscopy. Lung tumors from K-Ras^{G12D}/NF-κB animals are EGFP positive (Fig. 1B). Importantly, the lungs of K-Ras^{WT}/NF-κB mice have only a few scattered EGFP-positive cells (Fig. 1B). To rule out the possibility that the EGFP-positive cells within the lung tumors might be comprised of inflammatory cells (which are part of the tumor microenvironment and require NF-κB activation for their function; ref. 32), we performed GFP immunohistochemistry. As can be seen in Fig. 1C, many epithelial cells within the lung neoplastic lesions stain positive for EGFP (middle), whereas very few cells stain positive in K-Ras^{WT}/NF-κB mice (top). As expected, the lung neoplastic cells from K-Ras^{G12D}–positive mice lacking the EGFP reporter allele are negative for EGFP expression (bottom).

In addition to evaluating EGFP reporter activity, we measured levels of the phosphorylated form (phospho-Ser$^{32/36}$) of the IκBα protein, a marker of NF-κB and IKK activation (Fig. 1D). When compared with adenocre-infected K-Ras^{WT} lungs, the lungs of adenocre-infected K-Ras^{G12D} mice display increased levels of IκBα phosphorylation at Ser$^{32/36}$ coupled with lower levels of total IκBα protein (consistent with IKK-induced degradation). In addition, consistent with K-Ras activation, K-Ras^{G12D} mice display increased levels of phospho-AKT and phospho-p42/44. Finally, expression of the mutant 12D form of Ras was detected exclusively in K-Ras^{G12D} mice. These results support the EGFP analysis, indicating a higher degree of NF-κB activity in the lungs of K-Ras^{G12D} mice. Taken together, these results confirm that NF-κB is activated in K-Ras–induced murine lung tumors *in situ*.

Deletion of the NF-κB p65/RelA subunit in the mouse lung decreases K-Ras–induced lung tumorigenesis. Given that K-Ras–induced lung tumorigenesis triggers NF-κB activation, we asked if genetic deletion of the NF-κB subunit p65/RelA in the LSL K-Ras mouse model affects K-Ras–induced oncogenesis. To achieve p65/RelA inactivation, we

Downloaded from http://aacrjournals.org/cancerres/article-pdf/70/9/3537/2653977/3537.pdf by guest on 29 April 2025

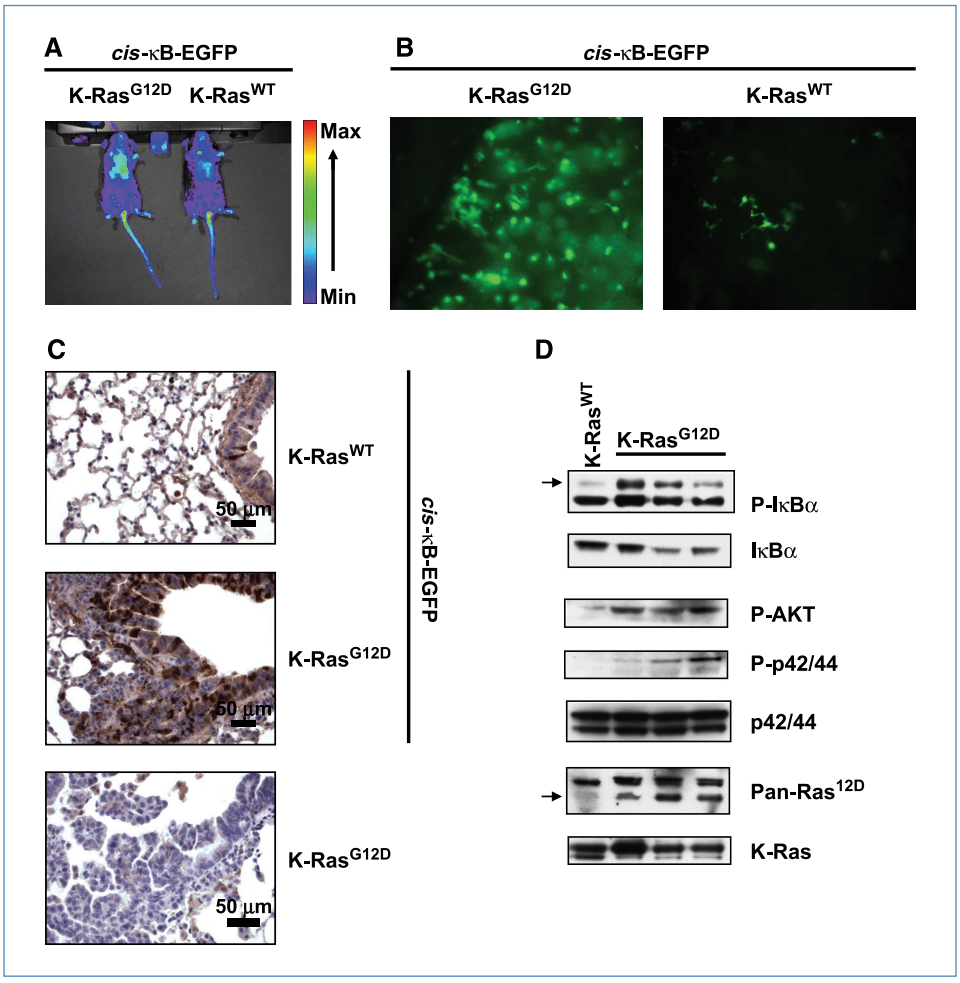

Figure 1. Oncogenic K-Ras activates NF-κB in lung tumors *in situ*. WT and K-Ras^{G12D}/NF-κB mice were analyzed 19 wks after infection. A, *in vivo* live EGFP fluorescence emission. Color scale indicates the range of fluorescence intensity. B, laser scanning microscopy of dissected lungs to measure EGFP fluorescence emission. C, lung tissue sections of WT and K-Ras^{G12D}/NF-κB mice were analyzed by GFP immunohistochemistry (positive cells stain in brown). Slides were counterstained with hematoxylin (blue). D, lung protein lysates from K-Ras^{G12D} or K-Ras^{WT} mice were submitted to Western blotting with the indicated antibodies. Arrows indicate the specific immunodetected bands; additional bands in blots are nonspecific.

bred the LSL K-Ras^{G12D} mice to p65$^{fl/fl}$ conditional mice (26) to obtain LSL K-Ras^{G12D}/p65$^{fl/fl}$ mice. Lungs were then infected with adenocre to activate K-Ras^{G12D} and inactivate p65/RelA simultaneously (K-Ras^{G12D}/p65$^{\Delta}$ mice).

As evaluated by pathologic examination of dissected lungs at 13 weeks postinfection, K-Ras^{G12D}/p65$^{\Delta}$ mice display a significantly reduced number of tumors than K-Ras^{G12D}/p65^{WT} mice (Fig. 2A). To confirm that recombination of the conditional p65/RelA allele occurred in the lungs of K-Ras^{G12D}/p65$^{\Delta}$ mice, we measured excision by PCR (see Fig. 2B). In addition, as revealed by immunohistochemical studies, the neoplastic lung lesions found in K-Ras^{G12D}/p65$^{\Delta}$ mice lacked p65/RelA expression (Fig. 2C). Interestingly, loss of p65/RelA affected not only the number of lesions formed but also their spread. As can be seen in Fig. 2D, most lesions formed in the presence of p65/RelA at 13 weeks postinfection have spread significantly into the alveolar compartment, whereas most lesions lacking p65/RelA at the same time point are still mostly contained within the bronchial epithelium. As these results indicate, although not absolutely required for tumor formation, p65/RelA greatly potentiates K-Ras–induced transformation in the lung *in situ*.

To gain insight into the role played by p65/RelA in potentiating K-Ras–induced oncogenesis, we investigated if loss of p65/RelA in this mouse model affects neoplastic cell survival. Relevant to this point, NF-κB has been shown, in cell-based studies, to be required to suppress Ras-induced apoptosis (21). Consistent with these previous findings, very few apoptotic cells were detected in K-Ras^{G12D}/p65^{WT} lesions, whereas a high number of apoptotic cells were seen in lesions of K-Ras^{G12D}/p65$^{\Delta}$ animals (Fig. 3).

The ability of the NF-κB p65/RelA subunit to potentiate K-Ras–induced lung tumorigenesis does not depend on the status of the p53 tumor suppressor. The tumor suppressor p53 is a well-known activator of the apoptotic response triggered upon oncogene activation; it is also known that p53 activity can be negatively regulated by NF-κB and vice versa (33). Therefore, it would be reasonable to assume that NF-κB can potentiate K-Ras–induced oncogenesis by suppressing p53 activity. However, contrary to this assumption, we showed that NF-κB regulates H-Ras–induced transformation in a p53-independent manner (21).

To address if p65/RelA potentiates K-Ras–induced oncogenesis by suppressing p53 activity, we generated a mouse model of K-Ras–induced lung cancer with combined loss of

Downloaded from http://aacrjournals.org/cancerres/article-pdf/70/9/3537/2653977/3537.pdf by guest on 29 April 2025

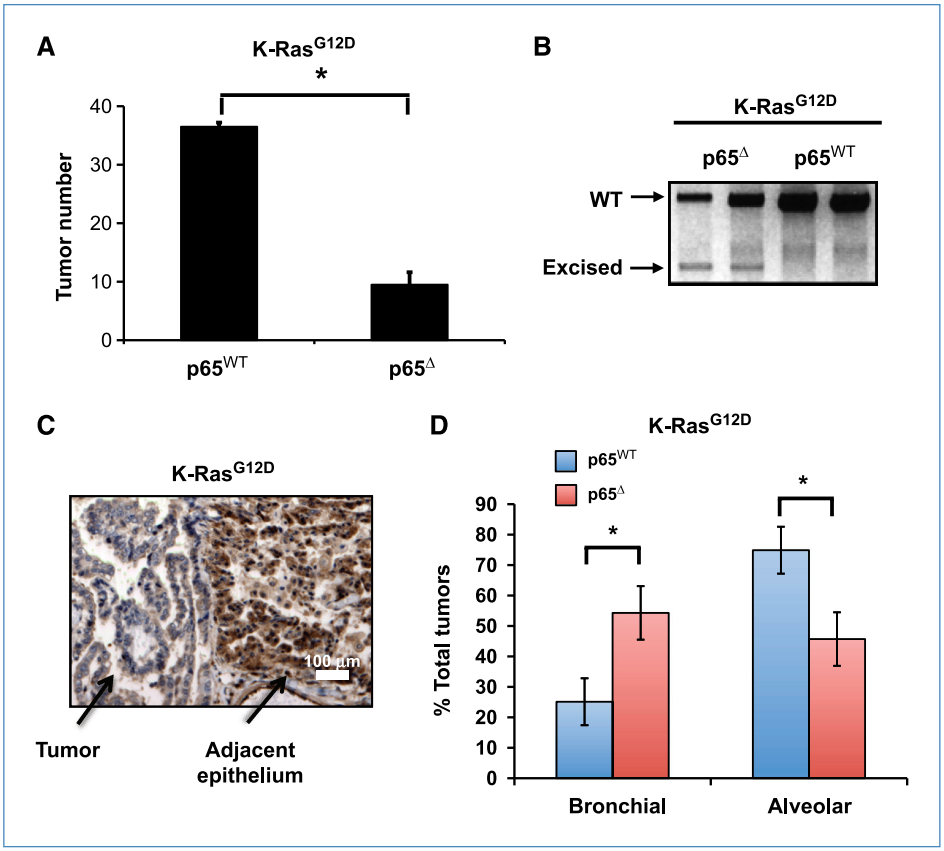

Figure 2. Loss of p65/RelA reduces formation and spread of K-Ras–induced lung tumors. K-Ras^{G12D}/p65^{WT} and K-Ras^{G12D}/p65$^{\Delta}$ mice were analyzed 13 wks after infection. A, number of K-Ras–induced neoplastic lesions was determined by counting lesions in H&E-stained lung sections as described (see Materials and Methods). B, PCR to detect Cre-mediated recombination of p65/RelA. Bands corresponding to the WT and excised alleles are indicated. C, immunohistochemistry for p65/RelA (positive cells are brown). Neoplastic lesion and adjacent epithelium are indicated. D, analysis of lung tumor spread was performed on H&E-stained lung sections as described (see Materials and Methods).

p65/RelA and p53 to ascertain whether loss of p53 would block the ability of p65/RelA to potentiate K-Ras transformation. For this purpose, we bred LSL K-Ras^{G12D}/p65$^{WT/WT}$ and LSL K-Ras^{G12D}/p65$^{fl/fl}$ models to p53$^{fl/fl}$ mice (27) to generate K-Ras^{G12D}/p53$^{\Delta}$/p65^{WT} and K-Ras^{G12D}/p53$^{\Delta}$/p65$^{\Delta}$ mice.

p53 is a strong tumor suppressor on its own, and its loss accelerates K-Ras tumor kinetics (29). We also observed this accelerated kinetics in animals with combined loss of p65 and p53. Although loss of p53 did not seem to affect the number of lesions formed, p53-null tumors grew faster and progressed to a higher histologic grade (data not shown). Nonetheless, similar to what was observed in K-Ras^{G12D} mice, loss of p65/RelA in K-Ras^{G12D}/p53$^{\Delta}$ mice resulted in a lower frequency of lung tumors (Fig. 4A). These data confirm previous cell-based studies (21), indicating that NF-κB potentiates K-Ras transformation in the lung independently of the status of p53.

Furthermore, loss of p65/RelA in K-Ras^{G12D}/p53$^{\Delta}$ mice resulted in lower-grade tumors. As outlined in Fig. 4B,

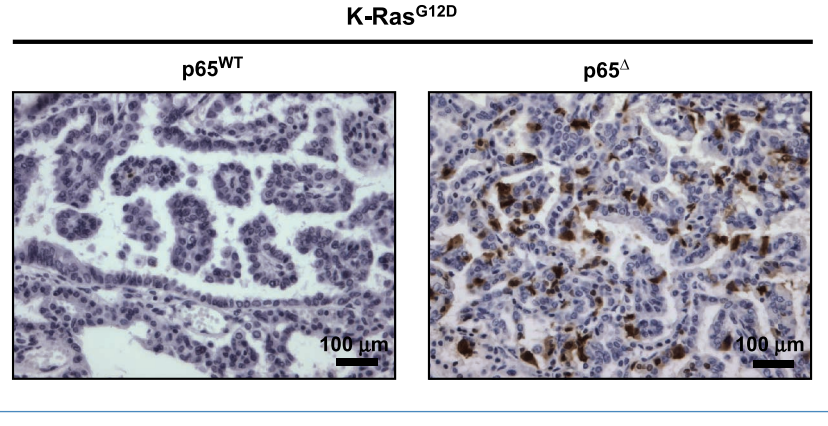

Figure 3. K-Ras^{G12D}/p65$^{\Delta}$ lung tumors have higher numbers of apoptotic cells. Apoptotic cells were detected by terminal deoxynucleotidyl transferase–mediated dUTP nick end labeling staining of lung tissue sections (positive cells are brown).

Downloaded from http://aacrjournals.org/cancerres/article-pdf/70/9/3537/2653977/3537.pdf by guest on 29 April 2025

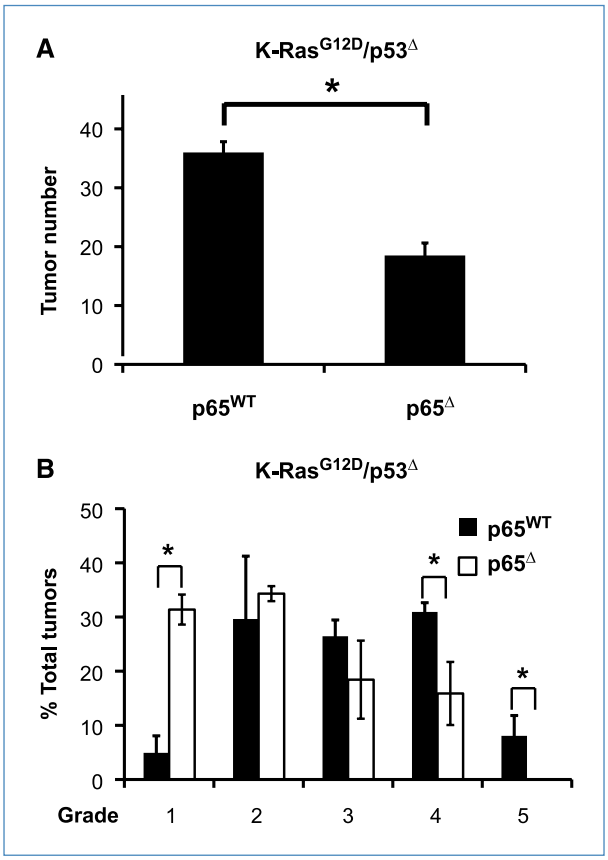

Figure 4. Loss of p65/RelA reduces formation and grade of K-Ras–induced lung tumors in the absence of p53. K-Ras^{G12D}/p53$^{\Delta}$/p65^{WT} and K-Ras^{G12D}/p53$^{\Delta}$/p65$^{\Delta}$ mice were analyzed 19 wks after infection. A, number of K-Ras–induced neoplastic lesions was determined by counting lesions in H&E-stained lung sections as described (see Materials and Methods). B, analysis of lung tumor grade was performed on H&E-stained lung sections as described (see Materials and Methods).

K-Ras^{G12D}/p53$^{\Delta}$/p65$^{\Delta}$ mice have a significantly higher percentage of grade 1 tumors than K-Ras^{G12D}/p53$^{\Delta}$/p65^{WT} mice. Conversely, Ras^{G12D}/p53$^{\Delta}$/p65$^{\Delta}$ mice have a significantly lower percentage of grade 4 and 5 tumors. This indicates that p65/RelA regulates not only survival of lung cells upon K-Ras activation but also other cell properties that contribute to progression of the malignant phenotype.

NF-κB is activated in human K-Ras–transformed lung epithelial cells, and activation requires IKKβ activity. The above experiments show that K-Ras activates NF-κB in the mouse lung, but it is important to confirm that the same relationship exists in human lung cells. Therefore, NF-κB activity was measured in low-passage primary immortalized human small airway cells (SALEB) and their K-Ras–transformed counterparts (SAKRAS; ref. 30). As can be seen in Fig. 5A, SAKRAS cells display p65-associated DNA binding activity (NF-κB band in untreated lane), whereas SALEB cells do not. SAKRAS cells also display increased sensitivity to cytokine-induced NF-κB activation (compare TNF lanes). In addition, when compared with SALEB cells, SAKRAS cells display highly elevated expression of NF-κB target genes *IL-8* and *MMP-9* and slightly elevated expression of Bcl-XL (Fig. 5B). Finally, similar to the murine lung tumors, SAKRAS cells also have increased levels of phospho-IκBα (Fig. 5C). Importantly, SAKRAS cells exhibit elevated phospho-IKK (Fig. 5C; see below).

In addition, we investigated NF-κB activity in H358 cells, a lung adenocarcinoma-derived cell line known to harbor a K-Ras oncogenic mutation (34). As shown in Fig. 6A (left), H358 cells exhibit constitutive NF-κB DNA binding activity that is suppressed upon siRNA-mediated knockdown of K-Ras expression, showing that the majority of NF-κB DNA binding activity in these cells is derived downstream of K-Ras expression.

Because of the increased level of phospho-IκBα detected in mouse tumors (Fig. 1D) and the increased levels of phosphorylated forms of both IκBα and IKKα/β in SAKRAS cells (Fig. 5C), we asked if NF-κB activation induced by K-Ras is mediated by IKK. First, we tested a potent IKKβ inhibitor (CmpdA; ref. 31) in SAKRAS cells. IKKβ inhibition, but not control treatment, blocked constitutive NF-κB DNA binding activity (Fig. 5A). Additionally, IKKβ inhibition blocked K-Ras–induced target gene expression (Fig. 5B).

We then explored siRNA knockdown to IKKβ in H358 cells. Knockdown of IKKβ strongly suppressed NF-κB DNA binding activity in H358 cells, similar to siRNA-mediated knockdown of K-Ras (Fig. 6A). Additionally, H358 cells were either transfected with a kinase-inactive version of IKKβ (IKKβ-KM) or treated with CmpdA, and NF-κB–dependent reporter activity was measured using luciferase. Results from these experiments show that both kinase-inactive IKKβ and CmpdA block NF-κB activity (Fig. 6B and C), indicating the involvement of IKK in the K-Ras–induced pathway. Finally, we investigated whether pharmacologic inhibition of IKKβ would also affect NF-κB activity in mouse cells. For this purpose, we used the KE67 cell line derived from lung tumors of our K-Ras^{G12D}/NF-κB EGFP reporter mice. As can be seen on Fig. 6D, treatment of KE67 cells with CmpdA reduced the number of EGFP-positive lung tumor cells by ~50%.

Taken together, these results indicate that IKKβ plays an important role in mediating NF-κB activation by K-Ras, supporting its inhibition in K-Ras–induced lung cancer as a potential new therapeutic approach.

Discussion

Point mutations in K-Ras occur frequently in lung cancer and drive the oncogenic phenotype. Because there are no effective therapies for K-Ras–positive lung cancer (or for lung cancer broadly), new approaches for therapy must be identified. In this regard, current interest is focused on downstream oncogenic effectors of the activated Ras forms (35–38). Previously, we had shown that the transcription factor NF-κB is critical for oncogenic transformation downstream of H-Ras (18, 21). Furthermore, trying to dissect the role of the NF-κB subunits in Ras transformation, our group also showed that the p65/RelA subunit contributes to efficient H-Ras–induced transformation (39). Additional studies

Downloaded from http://aacrjournals.org/cancerres/article-pdf/70/9/3537/2653977/3537.pdf by guest on 29 April 2025

have shown that p65/RelA is activated in tumor biopsies from K-Ras–induced lung cancer patients (20), in K-Ras–positive prostate epithelial cells (22), and in both pancreatic cancer cells and melanoma cells in a Ras-dependent manner (40, 41). Here, we have analyzed a role for the p65/RelA subunit of NF-κB downstream of oncogenic K-Ras for the development of lung tumors *in situ*.

Using LSL K-Ras^{G12D} mice (24), we show that K-Ras activates NF-κB in lung tumors *in situ* (Fig. 1). Recently, Meylan and colleagues (42) reported that NF-κB activation in the LSL K-Ras^{G12D} lung tumor model depends on deletion of p53. Our studies clearly show that NF-κB activation occurs when p53 is WT. Meylan and colleagues (42) analyzed nuclear accumulation of p65/RelA as a marker of NF-κB activation, whereas our studies used NF-κB–dependent EGFP reporter and IκBα phosphorylation from *in situ* tumors (Fig. 1). Thus, the use of distinct assays with different sensitivity likely explains the differences in findings from the two articles, specially as loss of p53 has been shown to further enhance NF-κB activation (43). More importantly, Meylan and colleagues (42) reported that expression of a degradation-resistant form of IκBα suppressed tumor formation in the K-Ras lung tumor model with deleted p53. Consistent with their findings, our results show that p65/RelA is needed for efficient lung tumor formation by K-Ras^{G12D} regardless of p53 status (Figs. 2 and 4).

Furthermore, consistent with the previous cell-based studies (21), Cre-generated deletion of p65/RelA in parallel with K-Ras^{G12D} activation led not only to reduced transformation (Fig. 2) but also to an apoptotic response in surviving tumors (Fig. 3). This result suggests that the reduction in lung tumor number in the p65/RelA-null setting is caused through an apoptotic response, with the surviving tumors presumably undergoing less (but measurable) apoptosis, which suggests that a likely mechanism for the role of p65/RelA in potentiating transformation is to promote cell survival. In this regard, we have not detected significant upregulation of traditional antiapoptotic genes by oncogenic H-Ras (39) or by K-Ras

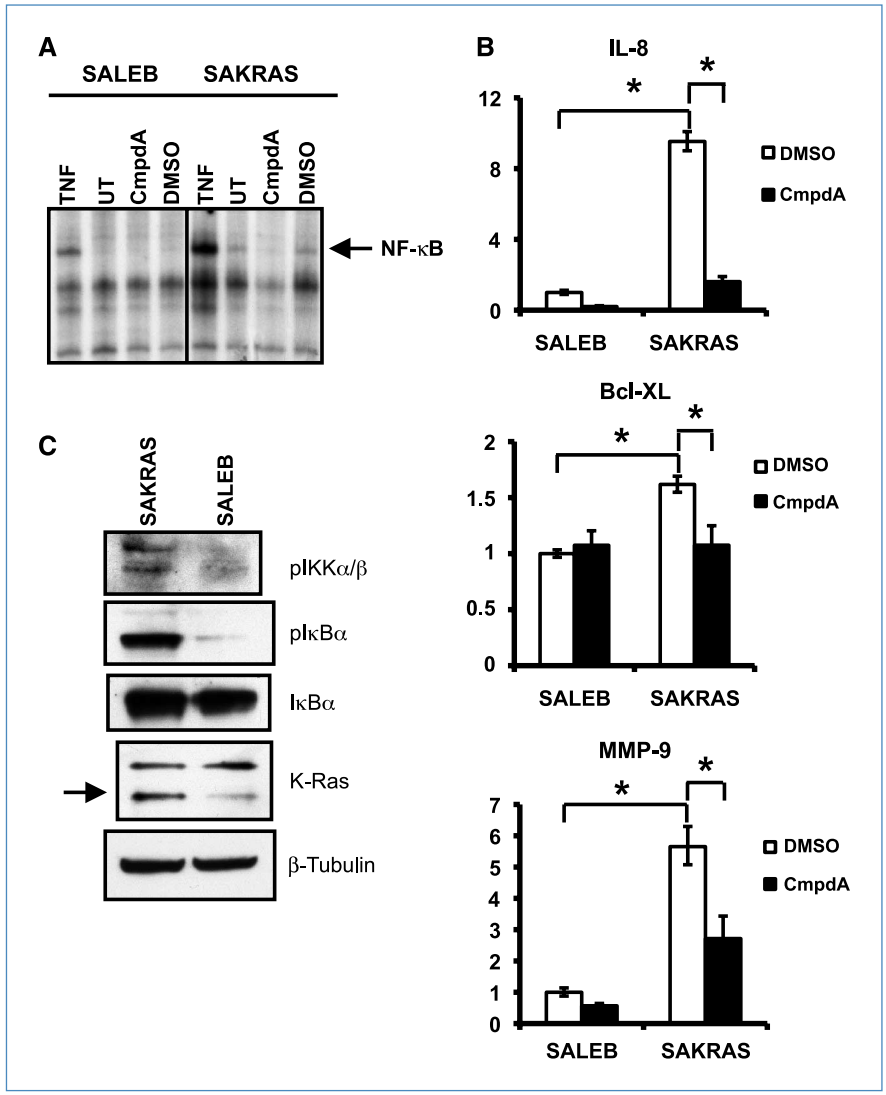

Figure 5. K-Ras–induced NF-κB activation in lung primary cells requires IKKβ activity. A, nuclear extracts of lung primary SALEB and SAKRAS cells were analyzed by EMSA with a probe containing a canonical NF-κB DNA binding site. Cells were either left untreated (UT) or treated for 1 h with 20 ng/mL tumor necrosis factor (TNF) α, 1 μmol/L CmpdA, or 0.02% DMSO. B, expression of NF-κB target genes *IL-8, Bcl-XL*, and *MMP-9* was analyzed by real-time quantitative PCR in SALEB and SAKRAS cells treated with 0.02% DMSO or 1 μmol/L CmpdA for 24 h. C, Western blotting of total protein lysates from SALEB or SAKRAS cells probed with different antibodies as indicated.

Downloaded from http://aacrjournals.org/cancerres/article-pdf/70/9/3537/2653977/3537.pdf by guest on 29 April 2025

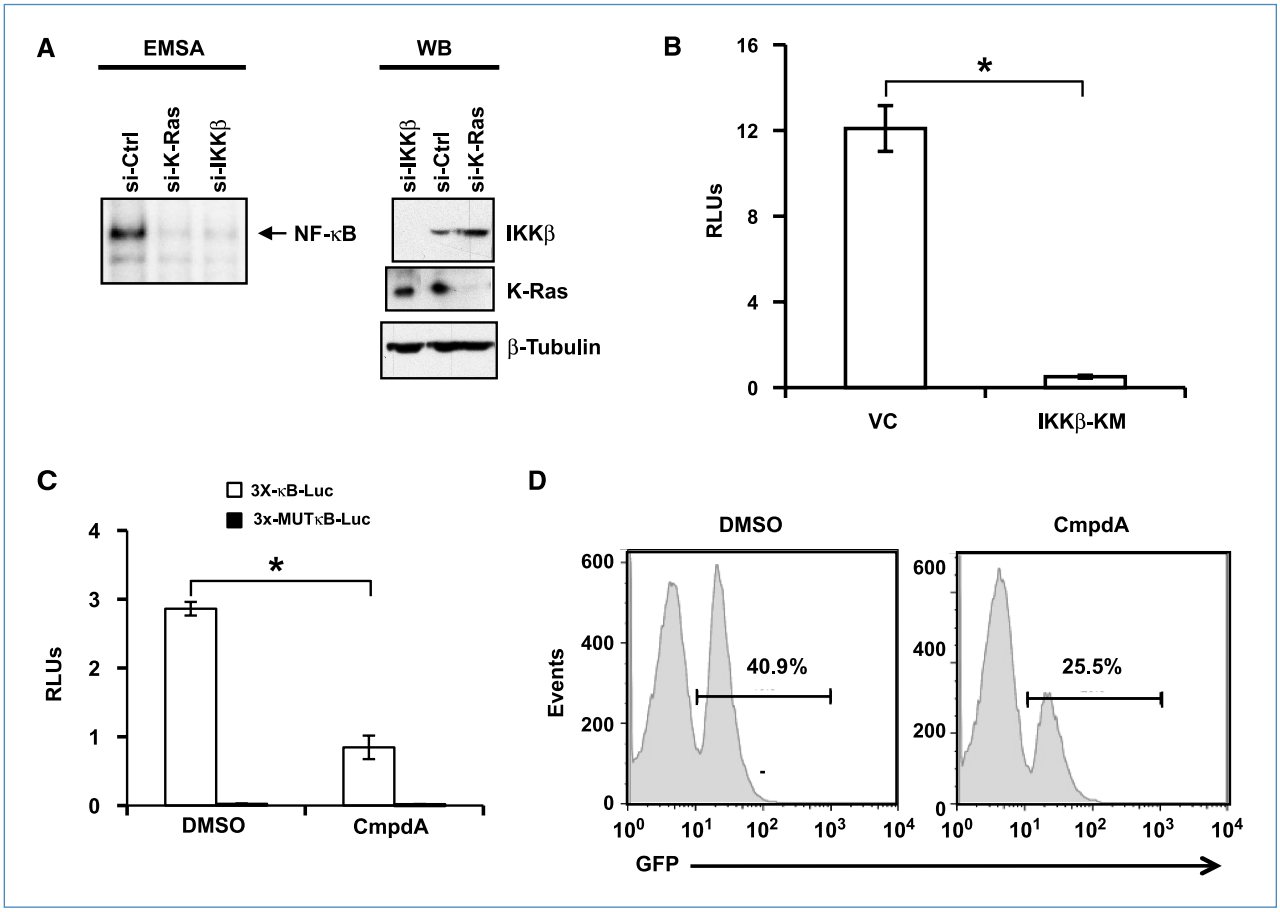

Figure 6. K-Ras–induced NF-κB activation in lung cancer cells requires IKKβ expression and activity. A, H358 cells were transiently transfected with siRNA targeted against K-Ras (si-K-Ras), IKKβ (si-IKKβ), and nontargeting control (si-Ctrl) and analyzed at 96 h after transfection for NF-κB DNA binding activity by EMSA (left) and efficiency of knockdown by Western blotting (WB; right). NF-κB DNA binding complexes as well as antibodies used are indicated. B and C, dual-luciferase reporter assays were performed using a NF-κB–responsive firefly luciferase reporter (3×-κB-Luc; white columns) or a NF-κB–unresponsive reporter (3×-MUTκB-Luc; black columns). B, H358 cells were transfected either with an empty pcDNA3 vector (VC) or with pcDNA3-IKKβ-KM. C, H358 cells were treated either with 0.02% DMSO or with 1 μmol/L CmpdA for 16 h. RLUs, relative light units. D, DMSO- or CmpdA-treated KE67 cells were analyzed by flow cytometry. Forward and side scatters were used to gate on live cells. The single-color histogram represents the number of events recorded in function of the level of GFP fluorescence emission using a logarithmic scale. A threshold for GFP-positive cells was arbitrarily set (linear gate), and the percentage of GFP-positive cells is indicated.

(Fig. 5B).[4] Future experiments will address mechanisms of survival controlled by p65/RelA downstream of oncogenic Ras expression.

The loss of p65/RelA significantly reduces, but does not eliminate, tumorigenesis downstream of oncogenic K-Ras expression (Figs. 2 and 4). We have previously shown that Ras-induced transformation is also impaired in c-Rel–null mouse embryonic fibroblasts (MEF) and that impairment is highest in c-Rel/p65 double-null MEFs (39), which suggests that both NF-κB subunits play an important role in Ras-mediated transformation. Consistent with our previous work, Barbie and colleagues (44) have shown that c-Rel expression is important for survival of K-Ras–transformed cells. Meylan and colleagues (42) have detected both c-Rel and p65/RelA activation in the LSL K-Ras^{G12D}/p53$^{\Delta}$ mouse model. These studies, together with the results described in this article, are consistent with a model where both NF-κB subunits would be activated by K-Ras to promote oncogenesis.

Although regulation of cell survival by p65/RelA certainly plays a role promoting K-Ras transformation, the reduced grade of p65/RelA-null K-Ras/p53$^{\Delta}$ lung tumors (Fig. 4B) suggests that p65/RelA regulates additional aspects of the malignant phenotype. Interestingly, in the panel of genes analyzed in human primary cells, the two most strongly K-Ras–induced genes were found to be *IL-8* and *MMP-9* (Fig. 5B), both of which are important in tumor progression. *IL-8* was shown to promote Ras-induced angiogenesis (45), and *MMP-9* has been shown to induce tumor invasion (46). Thus, in addition to controlling survival, NF-κB activation by oncogenic K-Ras likely involves additional oncogenic mechanisms, including enhanced invasion.

For therapy design purposes, it is important to identify mediators of K-Ras–induced NF-κB activation that can be

[4] Unpublished data.

Downloaded from http://aacrjournals.org/cancerres/article-pdf/70/9/3537/2653977/3537.pdf by guest on 29 April 2025

pharmacologically targeted. Here, we identify IKKβ as an important mediator of NF-κB activity in lung primary cells and lung cancer cell lines (Figs. 5 and 6). This is consistent with additional evidence that IKKβ is activated by oncogenic Ras (22, 23, 41, 47), as well as evidence that IKKβ promotes oncogenesis. Loss of IKKβ prevents tumorigenesis in a mouse model of colitis-associated cancer (48). Pharmacologic inhibition of IKKβ inhibits multiple myeloma cell growth *in vitro* and as xenograft tumors (49). Knockdown of IKKβ expression inhibits growth of H-Ras–driven melanomas (41). Finally, not only IKKβ activates mammalian target of rapamycin in certain breast cancer cells, thereby promoting tumor angiogenesis, but also its expression correlates with poor clinical outcome (50). Interestingly, the IKK-related kinase TBK1 has been recently implicated in K-Ras–induced transformation and NF-κB activation (44, 51). It remains to be determined whether IKKβ and TBK1 contribute to K-Ras–induced NF-κB activation independently or whether there is a functional connection between these two pathways. In this regard, TBK1 and IKKβ may contribute to different oncogenic phenotypes, with TBK1 serving as a stronger regulator of cancer cell survival.

In summary, our studies show that K-Ras triggers NF-κB activation in a mouse model of lung cancer *in situ*. NF-κB is an important K-Ras target in mediating the oncogenic process because loss of the NF-κB subunit p65/RelA significantly impairs lung tumor formation in the presence or absence of p53. In addition, inhibition of IKKβ expression or function blocks NF-κB activation in K-Ras–transformed lung cells, suggesting pharmacologic targeting of IKKβ or other upstream regulators that control NF-κB as a potential therapeutic approach for K-Ras–induced lung cancer therapy.

Disclosure of Potential Conflicts of Interest

No potential conflicts of interest were disclosed.

Acknowledgments

We thank Drs. Tyler Jacks and Christian Jobin for providing the LSL K-Ras^{G12D} and *cis*-κB-EGFP mice, respectively; Dr. Scott Randell for the kind gift of SALEB and SAKRAS cells; Dr. Gabriela Rozenberg for providing technical assistance with fluorescent microscopy; Dr. William Funkhouser for assistance with pathologic analysis; and the Baldwin laboratory members for insightful discussions and suggestions.

Grant Support

International Association for the Studies of Lung Cancer Fellowship, Doctor's Cancer Foundation, and a Young Clinical Scientist Award from the Flight Attendant Medical Research Institute (D.S. Basseres); Young Clinical Scientist Award from Flight Attendant Medical Research Institute (E. Levantini); and NIH grants CA73756 and CA75080, National Lung Cancer Partnership/LUNGevity Award, and Samuel Waxman Cancer Research Foundation (A.S. Baldwin).

The costs of publication of this article were defrayed in part by the payment of page charges. This article must therefore be hereby marked *advertisement* in accordance with 18 U.S.C. Section 1734 solely to indicate this fact.

Received 11/24/2009; revised 02/09/2010; accepted 02/23/2010; published OnlineFirst 04/20/2010.

References

1. Jemal A, Siegel R, Ward E, Hao Y, Xu J, Thun MJ. Cancer statistics, 2009. CA Cancer J Clin 2009;59:225–49.
2. Mills NE, Fishman CL, Rom WN, Dubin N, Jacobson DR. Increased prevalence of K-ras oncogene mutations in lung adenocarcinoma. Cancer Res 1995;55:1444–7.
3. Rodenhuis S, Slebos RJ. Clinical significance of ras oncogene activation in human lung cancer. Cancer Res 1992;52:2665–9s.
4. Slebos RJ, Rodenhuis S. The ras gene family in human non-small-cell lung cancer. J Natl Cancer Inst Monogr 1992:23–9.
5. Graziano SL, Gamble GP, Newman NB, et al. Prognostic significance of K-ras codon 12 mutations in patients with resected stage I and II non-small-cell lung cancer. J Clin Oncol 1999;17:668.
6. Herbst RS, Heymach JV, Lippman SM. Lung cancer. N Engl J Med 2008;359:1367–80.
7. Meuwissen R, Berns A. Mouse models for human lung cancer. Genes Dev 2005;19:643–64.
8. Schubbert S, Shannon K, Bollag G. Hyperactive Ras in developmental disorders and cancer. Nat Rev Cancer 2007;7:295–308.
9. Bossu P, Vanoni M, Wanke V, et al. A dominant negative RAS-specific guanine nucleotide exchange factor reverses neoplastic phenotype in K-ras transformed mouse fibroblasts. Oncogene 2000;19:2147–54.
10. Fleming JB, Shen G-L, Holloway SE, Davis M, Brekken RA. Molecular consequences of silencing mutant K-ras in pancreatic cancer cells: justification for K-ras-directed therapy. Mol Cancer Res 2005;3:413–23.
11. Shirasawa S, Furuse M, Yokoyama N, Sasazuki T. Altered growth of human colon cancer cell lines disrupted at activated Ki-ras. Science 1993;260:85–8.
12. Watanabe T, Shinohara N, Sazawa A, et al. Suppressive effects of dominant negative ras mutant N116Y on transformed phenotypes of human bladder cancer cells. Cancer Lett 2000;149:195–202.
13. Saxena N, Lahiri SS, Hambarde S, Tripathi RP. RAS: target for cancer therapy. Cancer Invest 2008;26:948–55.
14. Hayden MS, Ghosh S. Signaling to NF-κB. Genes Dev 2004;18:2195–224.
15. Yamamoto Y, Gaynor RB. IκB kinases: key regulators of the NF-κB pathway. Trends Biochem Sci 2004;29:72–9.
16. Perkins ND, Gilmore TD. Good cop, bad cop: the different faces of NF-κB. Cell Death Differ 2006;13:759–72.
17. Basseres DS, Baldwin AS. Nuclear factor-κB and inhibitor of κB kinase pathways in oncogenic initiation and progression. Oncogene 2006;25:6817–30.
18. Finco TS, Westwick JK, Norris JL, Beg AA, Der CJ, Baldwin AS. Oncogenic Ha-Ras-induced signaling activates NF-κB transcriptional activity, which is required for cellular transformation. J Biol Chem 1997;272:24113–6.
19. Reuther JY, Reuther GW, Cortez D, Pendergast AM, Baldwin AS. A requirement for NF-κB activation in Bcr-Abl-mediated transformation. Genes Dev 1998;12:968–81.
20. Tang X, Liu D, Shishodia S, et al. Nuclear factor-κB (NF-κB) is frequently expressed in lung cancer and preneoplastic lesions. Cancer 2006;107:2637–46.
21. Mayo MW, Wang C-Y, Cogswell PC, et al. Requirement of NF-κB activation to suppress p53-independent apoptosis induced by oncogenic Ras. Science 1997;278:1812–5.
22. Kim BY, Gaynor RB, Song K, Dritschilo A, Jung M. Constitutive activation of NF-κB in Ki-ras-transformed prostate epithelial cells. Oncogene 2002;21:4490–7.
23. Duran A, Linares JF, Galvez AS, et al. The signaling adaptor p62 is an important NF-κB mediator in tumorigenesis. Cancer Cell 2008;13:343–54.
24. Jackson EL, Willis N, Mercer K, et al. Analysis of lung tumor initiation and progression using conditional expression of oncogenic K-ras. Genes Dev 2001;15:3243–8.
25. Magness ST, Jijon H, Van Houten Fisher N, Sharpless NE, Brenner DA,

Downloaded from http://aacrjournals.org/cancerres/article-pdf/70/9/3537/2653977/3537.pdf by guest on 29 April 2025

Jobin C. *In vivo* pattern of lipopolysaccharide and anti-CD3-induced NF-κB activation using a novel gene-targeted enhanced GFP reporter gene mouse. J Immunol 2004;173:1561–70.
26. Steinbrecher KA, Harmel-Laws E, Sitcheran R, Baldwin AS. Loss of epithelial RelA results in deregulated intestinal proliferative/apoptotic homeostasis and susceptibility to inflammation. J Immunol 2008; 180:2588–99.
27. Jonkers J, Meuwissen R, van der Gulden H, Peterse H, van der Valk M, Berns A. Synergistic tumor suppressor activity of BRCA2 and p53 in a conditional mouse model for breast cancer. Nat Genet 2001;29: 418–25.
28. Wilson W, Baldwin AS. Maintenance of constitutive IκB kinase activity by glycogen synthase kinase-3α/β in pancreatic cancer. Cancer Res 2008;68:8156–63.
29. Jackson EL, Olive KP, Tuveson DA, et al. The differential effects of mutant p53 alleles on advanced murine lung cancer. Cancer Res 2005;65:10280–8.
30. Lundberg AS, Randell SH, Stewart SA, et al. Immortalization and transformation of primary human airway epithelial cells by gene transfer. Oncogene 2002;21:4577–86.
31. Ziegelbauer K, Gantner F, Lukacs NW, et al. A selective novel low-molecular-weight inhibitor of IκB kinase-β (IKK-β) prevents pulmonary inflammation and shows broad anti-inflammatory activity. Br J Pharmacol 2005;145:178–92.
32. Hagemann T, Biswas SK, Lawrence T, Sica A, Lewis CE. Regulation of macrophage function in tumors: the multifaceted role of NF-κB. Blood 2009;113:3139–46.
33. Tergaonkar V, Perkins ND. p53 and NF-κB crosstalk: IKKα tips the balance. Mol Cell 2007;26:158–9.
34. Yonesaka K, Zejnullahu K, Lindeman N, et al. Autocrine production of amphiregulin predicts sensitivity to both gefitinib and cetuximab in EGFR wild-type cancers. Clin Cancer Res 2008;14:6963–73.
35. Engelman JA, Chen L, Tan X, et al. Effective use of PI3K and MEK inhibitors to treat mutant Kras G12D and PIK3CA H1047R murine lung cancers. Nat Med 2008;14:1351–6.
36. Hamad NM, Elconin JH, Karnoub AE, et al. Distinct requirements for Ras oncogenesis in human versus mouse cells. Genes Dev 2002;16: 2045–57.
37. Lim KH, Baines AT, Fiordalisi JJ, et al. Activation of RalA is critical for Ras-induced tumorigenesis of human cells. Cancer Cell 2005;7: 533–45.
38. Rangarajan A, Hong SJ, Gifford A, Weinberg RA. Species- and cell type-specific requirements for cellular transformation. Cancer Cell 2004;6:171–83.
39. Hanson JL, Hawke NA, Kashatus D, Baldwin AS. The nuclear factor κB subunits RelA/p65 and c-Rel potentiate but are not required for Ras-induced cellular transformation. Cancer Res 2004;64:7248–55.
40. Liptay S, Weber CK, Ludwig L, Wagner M, Adler G, Schmid RM. Mitogenic and antiapoptotic role of constitutive NF-κB/Rel activity in pancreatic cancer. Int J Cancer 2003;105:735–46.
41. Yang J, Pan WH, Clawson GA, Richmond A. Systemic targeting inhibitor of κB kinase inhibits melanoma tumor growth. Cancer Res 2007;67:3127–34.
42. Meylan E, Dooley AL, Feldser DM, et al. Requirement for NF-κB signalling in a mouse model of lung adenocarcinoma. Nature 2009;462: 104–7.
43. Kawauchi K, Araki K, Tobiume K, Tanaka N. p53 regulates glucose metabolism through an IKK-NF-κB pathway and inhibits cell transformation. Nat Cell Biol 2008;10:611–8.
44. Barbie DA, Tamayo P, Boehm JS, et al. Systematic RNA interference reveals that oncogenic KRAS-driven cancers require TBK1. Nature 2009;462:108–12.
45. Sparmann A, Bar-Sagi D. Ras-induced interleukin-8 expression plays a critical role in tumor growth and angiogenesis. Cancer Cell 2004;6: 447–58.
46. Yang L, Zeng W, Li D, Zhou R. Inhibition of cell proliferation, migration and invasion by DNAzyme targeting MMP-9 in A549 cells. Oncol Rep 2009;22:121.
47. Arsura M, Mercurio F, Oliver AL, Thorgeirsson SS, Sonenshein GE. Role of the IκB kinase complex in oncogenic Ras- and Raf-mediated transformation of rat liver epithelial cells. Mol Cell Biol 2000;20: 5381–91.
48. Greten FR, Eckmann L, Greten TF, et al. IKKβ links inflammation and tumorigenesis in a mouse model of colitis-associated cancer. Cell 2004;118:285–96.
49. Hideshima T, Neri P, Tassone P, et al. MLN120B, a novel IκB kinase β inhibitor, blocks multiple myeloma cell growth *in vitro* and *in vivo*. Clin Cancer Res 2006;12:5887–94.
50. Lee DF, Kuo HP, Chen CT, et al. IKK β suppression of TSC1 links inflammation and tumor angiogenesis via the mTOR pathway. Cell 2007;130:440–55.
51. Chien Y, Kim S, Bumeister R, et al. RalB GTPase-mediated activation of the IκB family kinase TBK1 couples innate immune signaling to tumor cell survival. Cell 2006;127:157–70.

Downloaded from http://aacrjournals.org/cancerres/article-pdf/70/9/3537/2653977/3537.pdf by guest on 29 April 2025